HHS Public Access

Author manuscript

Otolaryngol Head Neck Surg. Author manuscript; available in PMC 2015 June 16.

Published in final edited form as:

Otolaryngol Head Neck Surg. 2014 October ; 151(4): 612–618. doi:10.1177/0194599814545083.

Matrix-Metalloproteinases in Head and Neck Carcinoma–Cancer Genome Atlas Analysis and Fluorescence Imaging in Mice

Samantha J. Hauff, MD[1,*], **Sharat C. Raju**[1,*], **Ryan K. Orosco, MD**[1], **Andrew M. Gross**[2], **Julio A. Diaz-Perez, MD**[1], **Elamprakash Savariar, PhD**[3], **Nadia Nashi**[1], **Jonathan Hasselman**[1], **Michael Whitney, PhD**[3], **Jeffrey N. Myers, MD**[4], **Scott M. Lippman, MD**[5], **Roger Y. Tsien, PhD**[3,6], **Trey Ideker, PhD**[2,7], and **Quyen T. Nguyen, MD, PhD**[1,5]

[1]Division of Head and Neck Surgery, University of California, San Diego, California, USA

[2]Bioinformatics and Systems Biology Program, University of California, San Diego, California, USA

[3]Department of Pharmacology, University of California, San Diego, California, USA

[4]Department of Head and Neck Surgery, University of Texas MD Anderson Cancer Center, Houston, Texas, USA

[5]Moores Cancer Center, University of California, San Diego, California, USA

[6]Howard Hughes Medical Institute, San Diego, California, USA

[7]Division of Medical Genetics, University of California, San Diego, California, USA

Abstract

Objective—(1) Obtain matrix-metalloproteinase (MMP) expression profiles for head and neck squamous cell carcinoma (HNSCC) specimens from the Cancer Genomic Atlas (TCGA). (2)

Corresponding Author: Quyen T. Nguyen, University of California San Diego, 9500 Gilman Drive, La Jolla, CA 92093, USA. quyennguyen@ucsd.edu.

*These authors contributed equally to this article.

Author Contributions

Samantha J. Hauff, design, conduct, analysis, manuscript preparation, and critical review; **Sharat C. Raju**, design, conduct, analysis, manuscript preparation, and critical review; **Ryan K. Orosco**, design, conduct, analysis, and critical review of data/manuscript; **Andrew M. Gross**, design, conduct, analysis, and critical review of data/manuscript; **Julio A. Diaz-Perez**, conduct, analysis, and critical review of figures/manuscript; **Elamprakash Savariar**, experimental design and critical review of manuscript; **Nadia Nashi**, conduct and critical review of data/text; **Jonathan Hasselman**, conduct, analysis, and critical review of figures/text; **Michael Whitney**, experimental design and critical review of manuscript; **Jeffrey N. Myers**, experimental design and critical review of manuscript; **Scott M. Lippman**, experimental design and critical review of manuscript; **Roger Y. Tsien**, experimental design, analysis, and critical review of manuscript; **Trey Ideker**, experimental design, analysis, and critical review of manuscript; **Quyen T. Nguyen**, design, analysis, manuscript preparation, and critical review.

Competing interests: Roger Y. Tsien, scientific advisor to Avelas Biosciences, which has licensed the ACPP technology from UCSD. Quyen T. Nguyen, scientific advisor to Avelas Biosciences, which has licensed the ACPP technology from UCSD.

Sponsorships: None.

This article will be presented at the 2014 AAO-HNSF Annual Meeting & OTO EXPO; September 21–24, 2014; Orlando, Florida.

Supplemental Material

Additional supporting information may be found at http://otojournal.org/supplemental.

Demonstrate HNSCC imaging using MMP-cleavable, fluorescently labeled ratiometric activatable cell-penetrating peptide (RACPP).

Study Design—Retrospective human cohort study; prospective animal study.

Setting—Translational research laboratory.

Subjects and Methods—Patient clinical data and mRNA expression levels of MMP genes were downloaded from TCGA data portal. RACPP provides complementary ratiometric fluorescent contrast (increased Cy5 and decreased Cy7 intensities) when cleaved by MMP2/9. HNSCC–tumor bearing mice were imaged in vivo after RACPP injection. Histology was evaluated by a pathologist blinded to experimental conditions. Zymography confirmed MMP-2/9 activity in xenografts. RACPP was applied to homogenized human HNSCC specimens, and ratiometric fluorescent signal was measured on a microplate reader for ex vivo analysis.

Results—Expression of multiple MMPs including MMP2/9 is greater in patient HNSCC tumors than matched control tissue. In patients with human papilloma virus positive (HPV+) tumors, higher MMP2 and MMP14 expression correlates with worse 5-year survival. Orthotopic tongue HNSCC xenografts showed excellent ratiometric fluorescent labeling with MMP2/9-cleavable RACPP (sensitivity = 95.4%, specificity = 95.0%). Fluorescence ratios were greater in areas of higher tumor burden (P <.03), which is useful for intraoperative margin assessment. Ex vivo, human HNSCC specimens showed greater cleavage of RACPP when compared to control tissue (P = .009).

Conclusions—Human HNSCC tumors show increased mRNA expression of multiple MMPs including MMP2/9. We used RACPP, a ratiometric fluorescence assay of MMP2/9 activity, to show improved occult tumor identification and margin clearance. Ex vivo assays using RACPP in biopsy specimens may identify patients who will benefit from intraoperative RACPP use.

Keywords

head and neck squamous cell carcinoma; fluorescence imaging; the Cancer Genomic Atlas; human papilloma virus

Introduction

Head and neck squamous cell carcinoma (HNSCC) is the sixth most common cancer worldwide with an estimated annual burden of 355,000 deaths and 633,000 incident cases.[1] Major risk factors include smoking, alcohol abuse, and human papilloma virus (HPV).[2] Surgical management is usually the primary therapy for this disease, although radiation and chemotherapy also have prominent roles.[3]

For HNSCC, matrix-metalloproteinase (MMP) expression has been shown to have prognostic value.[4–8] Of the various MMPs thought to be involved in cancer, attention has focused on MMPs 2 and 9 because they are overexpressed in a variety of malignant tumors, and their expression is often associated with tumor grade and poor patient prognosis. Absolute levels of MMP2/9 have been used to differentiate between benign papillomas and carcinoma of the larynx.[4] Increased MMP2/9 expression has also been shown to correlate with cancer grade[5] and decreased survival.[6,7] In carcinoma of the tongue, increased

MMP2/9 expression has been shown to correlate with an increased incidence of lymph node metastases.[8]

In this study, we sought to evaluate MMP mRNA levels in HNSCC using the Cancer Genomic Atlas (TCGA), the largest available collection of HNSCC specimens. We also evaluated the prognostic value of MMP mRNA levels in patients with HPV+ and HPV− HNSCC tumors.

Although MMP expression (mRNA and protein) has been associated with tumor grade and poor patient prognosis for a variety of cancers, at the tissue level, MMP activity is regulated by a variety of factors, including activation from pro-enzyme form and presence or absence of inhibitors.[9] Consequently, MMP activity, rather than expression, may have closer association with tumor biological behavior and therefore greater prognostic value. We have previously described activatable cell-penetrating peptides (ACPPs), which rely on tumor-associated proteases MMP2/9 to unmask the adhesiveness of CPPs.[10,11] We recently described a ratiometric version of ACPPs (RACPPs) that employs Cy5 as a far-red fluorescent resonance energy transfer (FRET) donor and Cy7 as near-infrared FRET acceptor. The Cy5 emission is absorbed by Cy7 and re-emitted as near-infrared fluorescence until the intervening linker is cleaved by tumor-associated MMP2/9. This cleavage event increases Cy5:Cy7 emission ratio up to 40-fold and enables tissue retention of the Cy5 fragment.[12] We have previously used ACPP to improve tumor margin (defined as tumor cells present at the cut edge of the surgical specimen) detection in animal model of melanoma and breast cancer.[13]

In HNSCC, positive margins have been associated with increased local recurrence and a poor prognosis.[14] For the majority of solid tumors, salvage surgery or adjuvant therapy not only cause extra trauma and expense but also often fail to remediate the poor outcome.[14–20] The reason for this observation is likely multifactorial and related in part to the difficulty in identifying the residual cancer during repeat surgery. Therefore, development of more sensitive imaging for accurate detection of positive surgical margins during the primary operation would be one of the most effective means to prevent positive margins, thereby minimizing patient suffering and expense while improving outcomes.

Using RACPP, we compared MMP2/9 activity levels between patient-derived ex vivo HNSCC specimens versus non-tumor tissue. We also evaluated the use of intravenously applied RACPPs to distinguish between orthotopic HNSCC xenografts from normal tissue and stratify tumor burden at the surgical margin in mice.

Methods

All animal studies were approved by the UCSD Institutional Animal Care and Use Committee. All studies involving tumor samples obtained from HNSCC patients were approved by the UCSD Institutional Review Board.

The Cancer Genomic Atlas

All available clinical and RNA expression data were downloaded from the TCGA data portal on December 15, 2013. HPV status was obtained from the TCGA HNSCC working group. HPV status was extracted from sequencing data or RNA data.[21] For tumor-normal comparison, 37 patients (out of 377 total) with matched tumor/normal tissue were considered and paired tests were used.

Ex Vivo Assay on HNSCC

Tumor samples were obtained from patients undergoing surgery for mucosal head and neck squamous cell carcinoma and stored at −80°C until analysis. Samples were homogenized using equal quantities of beads and tissue and twice the volume of phosphate buffered saline (PBS). One hundred fifty nmol of RACPP was added to 100 to 175 μl of PBS containing 25 μl of 10% tissue extract. Cleavage of the probe was determined by capturing the Cy5/Cy7 fluorescence ratio every 15 minutes for 2 hours (excitation 630 nm/emission 680–780 nm) using Tecan Infinite M100 pro plate reader (Tecan Laboratories, Switzerland).

Zymogram

Zymogram was prepared as previously described.[22] Briefly, 30 to 40 mg of tissue was homogenized in buffered solution and centrifuged. Tissue samples, along with SeeBlue Plus 2 Protein ladder and MMP standards, were loaded on the gel and run at 120 V for 2 hours. Following renaturation, development, and staining, gels were imaged and analyzed with Image J. MMP activity of samples was recorded as a percentage of MMP activity within the positive control lane.

Peptide Synthesis

RACPP and uncleavable-control were synthesized as previously described.[12] The RACPP contains a polycationic moiety linked to a neutralizing poly-anionic arm via a linker that is cleavable by MMP-2 and MMP-9. A Cy5 fluorophore is attached to the polycationic portion while the Cy7 fluorescent molecule is attached to the polyanionic domain. Following cleavage by MMPs, the polycationic portion conjugated to Cy5 is dequenched and becomes trapped within nearby tissue. Uncleavable-control peptide lacks an MMP cleavable linker.

Cell Culture and Mouse Tongue Xenografts

Human tongue squamous cell carcinoma lines SCC-4, SCC-9, SCC-15, and SCC-25 (ATCC) were maintained in Dulbecco's modified Eagle's medium with nutrient mixture F-12 (DMEM/ F-12) containing 10% fetal bovine serum (FBS) and supplemented with 400 ng/mL of hydrocortisone. Human tongue squamous cell carcinoma line CAL-27 (ATCC) was maintained in DMEM containing 10% FBS. Cells were incubated at 37°C in 5% CO_2. *Nu/nu* mice (age, 3–6 months) were injected with cultured HNSCC cells (~10^6 for CAL-27, ~5×10^6 for SCC-4, SCC-9, SCC-15, SCC-25) into the tip of the tongue. One cell line was used in each mouse for these experiments (n = 22 total; CAL-27: n = 5; SCC-25 n = 4; SCC-15: n = 4; SCC-4: n = 4; SCC-9: n = 5).

In Vivo Imaging with RACPP

Mice were monitored for 20% weight loss or tumor size >4–5 mm. Once these parameters were met, animals were anesthetized with isoflurane and injected intravenously with RACPP or control uncleavable peptide (0.4 nmol/g). Two hours after injection, mice were re-anesthetized (100 mg/kg ketamine and 5 mg/kg midazolam) and subcutaneous cervical tissue/anterior tongue exposed for imaging (Maestro, CRI, Guelph, Ontario, Canada). After completion of whole body imaging, animals were euthanized. The entirety of the tongue was immediately extracted and imaged in the dorsal position (Maestro).

Spectral imaging was carried out by exciting Cy5 at 620 (±10) nm followed by step-wise emission measurements from 640 to 840 nm through a tunable LCD emission filter. For ratio imaging, numerator (Cy5) and denominator (Cy7) images were generated by integrating spectral images over a defined range at 10 nm intervals (660–720 nm for Cy5 and 760–830 nm for Cy7). Ratio images were generated and color-encoded using custom software. The ratio for each pixel was encoded as hue on a blue to red scale, and brightness was based on the original Cy5 images. The software also generated monochromatic Cy5/Cy7 images for further processing (see image analysis and histologic correlation).

Histology

Immediately following imaging, tongue tissues were embedded in cryopreservative and stored at −80°C. Samples were cryosectioned into 5-μM sections in the same orientation as the whole tongue molecular imaging and stained with hematoxylin and eosin (H&E). The entirety of the tongue was included in the slice, including both tumor and normal tissue. Samples were evaluated by a pathologist blinded to experimental conditions.

Mapping Histology to Molecular Imaging

For histologic samples, a pathologist blinded to experimental conditions used a stage micrometer to determine the tumor's linear position and extent along the length of the tongue. This information was mapped to spectral images of the tongue. A mean Cy5/Cy7 ratio was calculated for segments containing histologically confirmed tumor and, separately, tumor-free segments.

Percentage tumor involvement was approximated by the pathologist as the density of cancerous tissue (vs non-cancerous tissue) within the tumor-containing segment of tongue. For example, if the tumor-bearing length of the sample contained only malignant cells and no normal tissue, percentage involvement was recorded as 100%. If only half of this region contained malignancy, percentage involvement was recorded as 50%. This method for calculating percentage tumor involvement has been utilized in other studies.[23,24]

Image Processing and Ratio Calculations

Monochromatic Cy5 and Cy7 images were extracted from the spectral image using custom software. Using the "Image Calculator" feature on Image J, the Cy5 image was divided by the Cy7 image to produce a new image, where Cy5/Cy7 ratios were encoded by pixel intensity. Ratios were calculated separately for tumor and normal tongue, which were

distinguished based on the histologic map described previously. These ratios were each normalized to Cy5/Cy7 ratios of background tissue (cervical soft tissue).

Statistics

Statistical analysis between experimental groups was conducted using either the 2-tailed independent sample Student's *t* test or one-way ANOVA with post hoc analysis. Graphical bar-plots were produced using Microsoft Excel, while receiver-operating curve (ROC) curves were created with Sigmaplot (12.3). Paired tests were used for TCGA analysis due to matched expression data. For survival analysis, Cox proportional hazards regression was employed using the R "survival" package.

Results

MMPs Are Overexpressed in HNSCC

To evaluate MMP expression levels in HNSCC from the TCGA, we compared patient-derived tumor specimens with matched normal control tissue. TCGA profiled matched normal tissue for approximately 10% of the patients (37 of 377). Thus, these data were used in our analysis. HNSCC tumors showed increased expression of multiple MMPs compared to matched control non-tumor tissue (Figure 1A, all P values < .01). Interestingly, MMP14 (also known as MT1-MMP) was the protease with the highest total expression in tumor tissue and had significantly higher expression in tumor compared to matched control tissue ($P < 10^{-5}$). The second highest expressing MMP in tumor tissue was MMP2. MMP2 and 9 share a common cleavage sequence, and they have been particularly well characterized in prior studies in association with HNSCC.[25] We found that both MMP2 ($P < 10^{-10}$) and MMP9 ($P < 10^{-6}$) have significantly greater RNA expression in HNSCC tumors compared to paired-control tissue (n = 37; 34 HPV− and 3 HPV+, Wilcoxon signed-rank test).

MMP 2 and 14 Stratify Survival in HPV+ HNSCC

Next, we evaluated the difference in MMP expression between HPV+ and HPV− tumors. We found that HPV+ tumors had less overall MMP expression compared to HPV− tumors (Figure 1B, Kruskal-Wallis test on pooled RNA levels, $P < 10^{-10}$). This is consistent with the hypothesis that HPV+ tumors are less biologically aggressive and consequently that these patients tend to have improved survival compared to patients with HPV− tumors. Interestingly, we found that in patients with HPV+ HNSCC, increased expression levels of MMP2 and MMP14 correlated with worse survival (Figures 1C, 1D, $P < .01$). Patients with HPV+ tumors who have the highest MMP2 and MMP14 expression (Figures 1C, 1D red lines) had significantly worse 5-year survival compared to patients with the lowest expression levels of these proteases (Figures 1C, 1D blue lines). Additionally, for a given patient with HPV+ tumor, there is a significant correlation between MMP2 and MMP14 expression (Supplemental Figure S1, available at www.otojournal.org, Spearman Rho = 0.56, $P < 10^{-4}$). Thus, poor prognosis HPV+ tumors stratified in the highest quartiles of MMP2 expression are also likely to have higher expression of MMP14. We did not find the same correlation in MMP expression with survival in patients with HPV–tumors. The cause of this is multifactorial and likely related to the observation that HPV− tumors have more genetic mutations compared HPV+ tumors.[26]

Zymography

To confirm MMP2/9 activity in mouse HNSCC xenografts, we measured cleavage of gelatin by tumor homogenates via zymography. We found a 2-fold increase in MMP9 and a 13-fold increase in MMP2 activity in HNSCC xenografts compared to normal mouse tongue tissue (Supplemental Figure S2, available at www.otojournal.org).

RACPP in ex Vivo HNSCC

To evaluate ex vivo MMP2/9 activity in human and mouse HNSCC specimens, we measured the maximum rate of Cy5/Cy7 ratio change over time in homogenates following addition of RACPP (Figures 2A, 2B). We found that patient-derived HNSCC specimens show higher MMP2/9 activity compared to non-tumor tissue (Figure 2C) (ROC analysis: area under the curve [AUC] = 1.000, $P = .01$). Similarly, mouse HNSCC xenografts also show higher Cy5/Cy7 rate change, signifying higher MMP2/9 activity compared to non-tumor tissue (ROC analysis: AUC = 1.000, $P = .03$).

RACPP Improves Detection of HNSCC

To test tumor-dependent Cy5/Cy7 ratiometric change in living mice, we intravenously injected tongue tumor bearing *nu/nu* mice with RACPP (n = 25). We conducted multispectral imaging of these live, anesthetized mice (ex 620, em 640–840 nm, Maestro, at 2 hours after injection) with both tongue and subcutaneous cervical tissue exposed (Figure 3A). We then excised the tongue and performed multispectral imaging of the tongue. Histologic information regarding tumor location and size was correlated and mapped to ratiometric fluorescence image of the tongue. Sample (tumor and non-tumor tissue) Cy5/Cy7 ratios were divided by "background" subcutaneous cervical tissue Cy5/Cy7 ratio to compute a "normalized Cy5/Cy7 ratio."[12]

We found higher Cy5/Cy7 ratiometric fluorescence in tumor (Figure 3B, red color) compared to adjacent normal tongue (Figure 3B, tan color). Injections of our control (uncleavable) probe revealed no ratiometric difference between tongue tumor and normal tongue (Figure 3C). Following intravenous administration of MMP2/9-cleavable RACPP, mice showed greater normalized Cy5/Cy7 ratio in tumor (1.61 ± 0.05, n = 22) compared to normal tongue (1.11 ± 0.03, n = 20, $P < 10^{-8}$). This increase in ratiometric fluorescence in orthotopic tumors was not seen following intravenous injection of uncleavable control probe (tumor = 1.01 ± 0.04, n = 3; normal tongue = 1.07 ± 0.03, n = 3, $P = .30$) (Figure 3D).

The ROC for cleavable RACPP revealed an AUC of 0.995 ± 0.006 ($P < 10^{-4}$) with a peak sensitivity of 95% and peak specificity of 100% for a normalized ratio cutoff of 1.345 (Figure 3D insert). The 2 tumor specimens not detected by this threshold cutoff had relatively low tumor burden (<60% involvement, see the following).

RACPPs Enable Stratification of Tumor Burden

One critical component of intraoperative margin evaluation is determining how much tumor burden is present at the edges of the surgical field. To evaluate the ability of RACPP to stratify tissue with variable tumor burden, percentage involvement of cancer within tumor-bearing portions of each sample was approximated by a pathologist blinded to experimental

conditions. We found varying levels of tumor burden among the 22 samples ranging from 25% to 100% invasion (Figure 4A). To evaluate the stratification of ratiometric fluorescence values between different levels of tumor burden, samples were statistically separated into the following tertiles of cancer involvement: 25% to 60% (n = 8), 61% to 80% (n = 8), and 81% to 100% (n = 6) (Figure 4B). Adjusted Cy5/Cy7 ratios were computed for each tertile and compared with normal tongue tissue (n = 20).

We found that all tertiles of varying tumor burden showed significantly greater normalized Cy5/Cy7 ratio than normal tongue tissue (Figure 4C; lowest tertile of tumor involvement = 1.46 ± 0.07, $P < 10^{-5}$; middle tertile = 1.67 ± 0.12, $P < 10^{-7}$; highest tertile = 1.72 ± 0.04, $P < 10^{-7}$). Additionally, tumors with percentage involvement in the highest and middle tertiles showed significantly greater normalized ratios than the lowest tertile ($P = .01$ for highest vs lowest tertile, $P = .03$ for middle vs lowest tertile). Future experiments will focus on evaluating the ability of RACPP to detect incrementally smaller levels of tumor burden (ie, from 1% to 25% involvement).

Discussion

In this study, we analyzed mRNA expression levels for MMPs in human HNSCC using the Cancer Genomic Atlas, the largest available collection of human HNSCC specimens. We also evaluated the prognostic value of MMP overexpression in terms of survival in patients with HPV+ and HPV− HNSCC tumors. We found that many MMPs are overexpressed in HNSCC tumors compared to paired control tissue. However, patients with HPV+ HNSCC tumors have significantly lower overall MMP levels compared to patients with HPV− HNSCC tumors. This finding is consistent with previous studies showing that patients with HPV+ HNSCC tumors have better overall survival compared to patients with HPV− HNSCC tumors.[27]

Of the various MMPs thought to be involved in cancer, attention has focused on MMP2/9 because they are overexpressed in a variety of malignant tumors and their expression is often associated with tumor grade and poor patient prognosis. Interestingly, we found that of the MMPs that are increased in tumor compared to control tissue, MMP2 and MMP14 are expressed at higher levels compared to all other MMPs, suggesting that these proteinases may be particularly important in HNSCC. Furthermore, we found that in patients with HPV + HNSCC tumors, increased MMP2 and MMP14 expression levels correlated with worse overall survival. If clinically validated in a prospective trial, the increases in MMP2 and MMP14 represent 2 molecular biomarkers that can individualize management of patients with HPV+ tumors.

Using MMP2/9 cleavable RACPP, we found that ex vivo human HNSCC specimens show greater activity compared to normal tissue. This finding correlates with previous studies demonstrating higher MMP2/9 expression at the invasive edge of tumors.[28] The high sensitivity and specificity of RACPPs to differentiate between tumor and normal tissue suggests that ex vivo measurements of MMP2/9 activity in HNSCC specimens may complement MMP mRNA expression studies in evaluating patient prognosis and in determining which patients would benefit from RACPP guided surgery.

In multiple human cell line models of HNSCC xenografts, we found higher MMP2/9 activity as evidenced by gelatinase zymography and higher ratiometric fluorescence signal following systemically applied RACPP compared to non-tumor tissue. All ratios were computed from histologically confirmed tumor or normal tissue, eliminating verification bias. The ideal discrimination threshold for detecting cancer versus normal tissue is 1.345, which is consistent with previously reported ratiometric thresholds for this probe.[12] Our study tested multiple tongue squamous cell carcinoma cell lines from ATCC to highlight the RACPP's broad applicability.

One critical component of intraoperative margin evaluation is determining how much tumor burden is present at the edges of the surgical field. We found that within tumor bearing tissue, the greater the tumor burden, the greater the ratiometric fluorescence signal following intravenous RACPP administration. Percentage tumor involvement has been shown to be important for survival and recurrence outcomes in prostate and breast cancer.[23,29] The correlation between intraoperative ratiometric fluorescence level and tumor burden suggests that RACPP can improve intraoperative decision making by providing information regarding local level of tumor involvement and consequently margin clearance.

Supplementary Material

Refer to Web version on PubMed Central for supplementary material.

Acknowledgments

The authors would like to thank Paul Steinbach for assistance with Maestro and fluorescence imaging, Perla Arcaira for animal handling, Joan Kanter for administrative and logistical assistance, and lab members for helpful discussion.

Funding source: Burroughs-Wellcome Fund (CAMS) and NIH (NCI) P50 CA097007 Developmental Research Program to QTN; CA and BCRP grants to RYT; NIH T32 Grant to SJH; NIH TL1 Grant (RR031979) to SCR.

References

1. Ferlay J, Shin HR, Bray F, Forman D, Mathers C, Parkin DM. Estimates of worldwide burden of cancer in 2008: GLOBOCAN 2008. Int J Cancer. 2010; 127:2893–2917. [PubMed: 21351269]
2. D'Souza G, Kreimer AR, Viscidi R, et al. Case-control study of human papillomavirus and oropharyngeal cancer. N Engl J Med. 2007; 356:1944–1956. [PubMed: 17494927]
3. Shin DM, Khuri FR. Advances in the management of recurrent or metastatic squamous cell carcinoma of the head and neck. Head Neck. 2013; 35:443–453. [PubMed: 22052826]
4. Uloza V, Liutkevicius V, Pangonyte D, Saferis V, Lesauskaite V. Expression of matrix metalloproteinases (MMP-2 and MMP-9) in recurrent respiratory papillomas and laryngeal carcinoma: clinical and morphological parallels. Eur Arch Otorhinolaryngol. 2011; 268:871–878. [PubMed: 21259063]
5. Wittekindt C, Jovanovic N, Guntinas-Lichius O. Expression of matrix metalloproteinase-9 (MMP-9) and blood vessel density in laryngeal squamous cell carcinomas. Acta Otolaryngol. 2011; 131:101–106. [PubMed: 20873997]
6. Liu WW, Zeng ZY, Wu QL, Hou JH, Chen YY. Overexpression of MMP-2 in laryngeal squamous cell carcinoma: a potential indicator for poor prognosis. Otolaryngol Head Neck Surg. 2005; 132:395–400. [PubMed: 15746850]

7. Mallis A, Teymoortash A, Mastronikolis NS, Werner JA, Papadas TA. MMP-2 expression in 102 patients with glottic laryngeal cancer. Eur Arch Otorhinolaryngol. 2012; 269:639–642. [PubMed: 21667117]
8. Zhou CX, Gao Y, Johnson NW, Gao J. Immunoexpression of matrix metalloproteinase-2 and matrix metalloproteinase-9 in the metastasis of squamous cell carcinoma of the human tongue. Aust Dent J. 2010; 55:385–389. [PubMed: 21174909]
9. Chaudhary AK, Singh M, Bharti AC, et al. Genetic polymorphisms of matrix metalloproteinases and their inhibitors in potentially malignant and malignant lesions of the head and neck. J Biomed Sci. 2010; 17:10. [PubMed: 20152059]
10. Olson ES, Aguilera TA, Jiang T, et al. In vivo characterization of activatable cell penetrating peptides for targeting protease activity in cancer. Integr Biol (Camb). 2009; 1:382–393. [PubMed: 20023745]
11. Aguilera TA, Olson ES, Timmers MM, Jiang T, Tsien RY. Systemic in vivo distribution of activatable cell penetrating peptides is superior to cell penetrating peptides. Integr Biol. 2009; 1:371–381.
12. Savariar EN, Felsen CN, Nashi N, et al. Real-time in vivo molecular detection of primary tumors and metastases with ratiometric activatable cell-penetrating peptides. Cancer Res. 2013; 73:855–864. [PubMed: 23188503]
13. Nguyen QT, Olson ES, Aguilera TA, et al. Surgery with molecular fluorescence imaging using activatable cell-penetrating peptides decreases residual cancer and improves survival. Proc Natl Acad Sci U S A. 2010; 107(9):4317–4322. [PubMed: 20160097]
14. Haque R, Contreras R, McNicoll MP, Eckberg EC, Petitti DB. Surgical margins and survival after head and neck cancer surger. BMC Ear Nose Throat Disord. 2006; 16:2. [PubMed: 16503981]
15. Singletary S. Surgical margins in patients with early-stage breast cancer treated with breast conservation therapy. Am J Surg. 2002; 184:383–393. [PubMed: 12433599]
16. Nagtegaal ID, Quirke P. What is the role for the circumferential margin in the modern treatment of rectal cancer? J Clin On. 2008; 26:303–312.
17. Meric F, Mirza N, Vlastos G, et al. Positive surgical margins and ipsilateral breast tumor recurrence predict disease-specific survival after breast-conserving therapy. Cancer. 2003; 97:926–933. [PubMed: 12569592]
18. Snijder R, de la Riviere A, Elbers H, van den Bosch J. Survival in resected stage I lung cancer with residual tumor at the bronchial resection margin. Ann Thorac Surg. 1998; 65:212–216. [PubMed: 9456120]
19. Dotan Z, Kavanagh K, Yossepowitch O, et al. Positive surgical margins in soft tissue following radical cystectomy for bladder cancer and cancer specific survival. J Urol. 2007; 178:2308–2312. [PubMed: 17936804]
20. Wieder JA, Soloway MS. Incidence, etiology, location, prevention and treatment of positive surgical margins after radical prostatectomy for prostate cancer. J Urol. 1998; 160:299–315. [PubMed: 9679867]
21. Gross A, Orosco R, Shen J, et al. A prognostic model of head and neck cancer ties TP53 mutation to 3p loss. Nature Genetics. In Press.
22. Toth M, Sohail A, Fridman R. Assessment of gelatinases (MMP-2 and MMP-9) by gelatin zymography. Methods Mol Biol. 2012; 878:121–135. [PubMed: 22674130]
23. Rampersaud EN, Sun L, Moul JW, Madden J, Freedland SJ. Percent tumor involvement and risk of biochemical progression after radical prostatectomy. J Urol. 2008; 180:571–576. [PubMed: 18554662]
24. Thompson IM III, Salem S, Chang SS, et al. Tumor volume as a predictor of adverse pathologic features and biochemical recurrence (BCR) in radical prostatectomy specimens: a tale of two methods. World J Urol. 2011; 29:15–20. [PubMed: 21079968]
25. Xia T, Akers K, Eisen AZ, Seltzer JL. Comparison of cleavage site specificity of gelatinases A and B using collagenous peptides. Biochim Biophys Acta. 1996; 1293:259–266. [PubMed: 8620038]
26. Maruyama H, Yasui T, Ishikawa-Fujiwara T, et al. Human papillomavirus and p53 mutations in head and neck squamous cell carcinoma among Japanese population. Cancer Sci. 2014; 105(4): 409–417. [PubMed: 24521534]

27. Sivars L, Nasman A, Tertipis N, et al. Human papillomavirus and p53 expression in cancer of unknown primary in the head and neck region in relation to clinical outcome. Cancer Med. 2014; 3:376–384. [PubMed: 24510528]

28. Kuniyasu H, Troncoso P, Johnston D, et al. Relative expression of type IV collagenase, E-cadherin, and vascular endothelial growth factor/vascular permeability factor in prostatectomy specimens distinguishes organ-confined from pathologically advanced prostate cancers. Clin Cancer Res. 2000; 6:2295–2308. [PubMed: 10873080]

29. Kohrt HE, Nouri N, Nowels K, Johnson D, Holmes S, Lee PP. Profile of immune cells in axillary lymph nodes predicts disease-free survival in breast cancer. PLoS Med. 2005; 2:e284. [PubMed: 16124834]

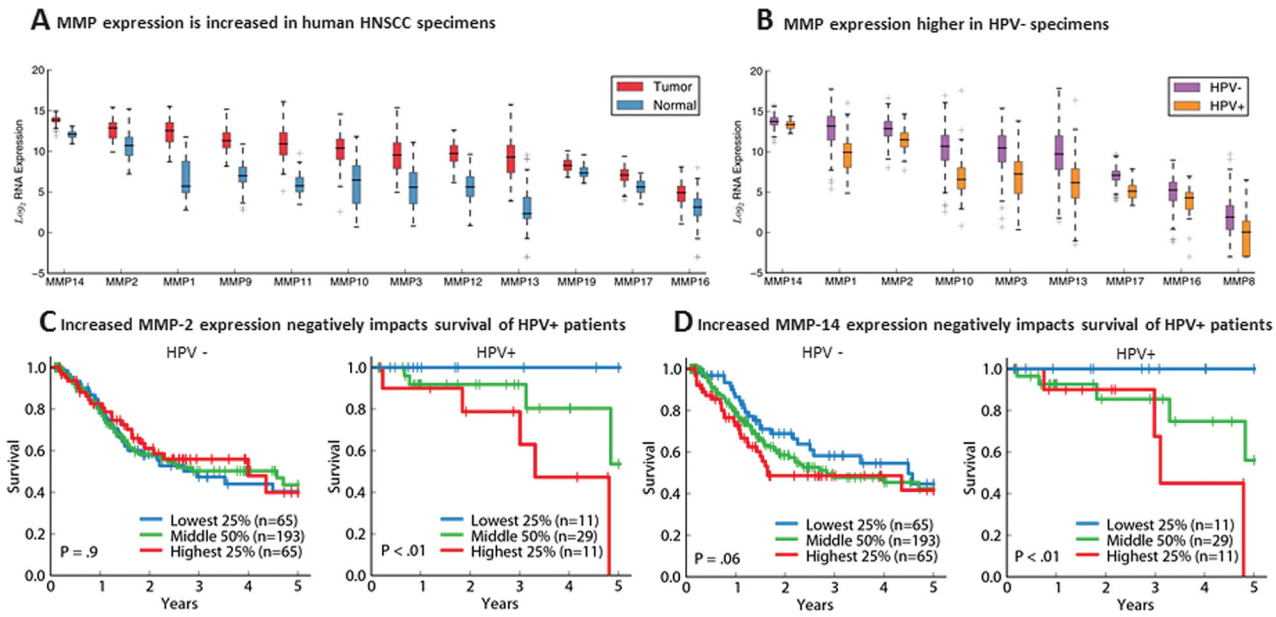

Figure 1.

(A) Higher MMP expression in tumors versus normal tissue in TCGA HNSCC. (B) HPV+ tumors have lower MMP expression than HPV− tumors. (C, D) Higher MMP-2/MMP-14 expression in HPV+ tumors correlates with poorer prognosis. Abbreviations: MMP, matrix-metalloproteinase; TCGA, the Cancer Genomic Atlas; HNSCC, head and neck squamous cell carcinoma; HPV, human papilloma virus.

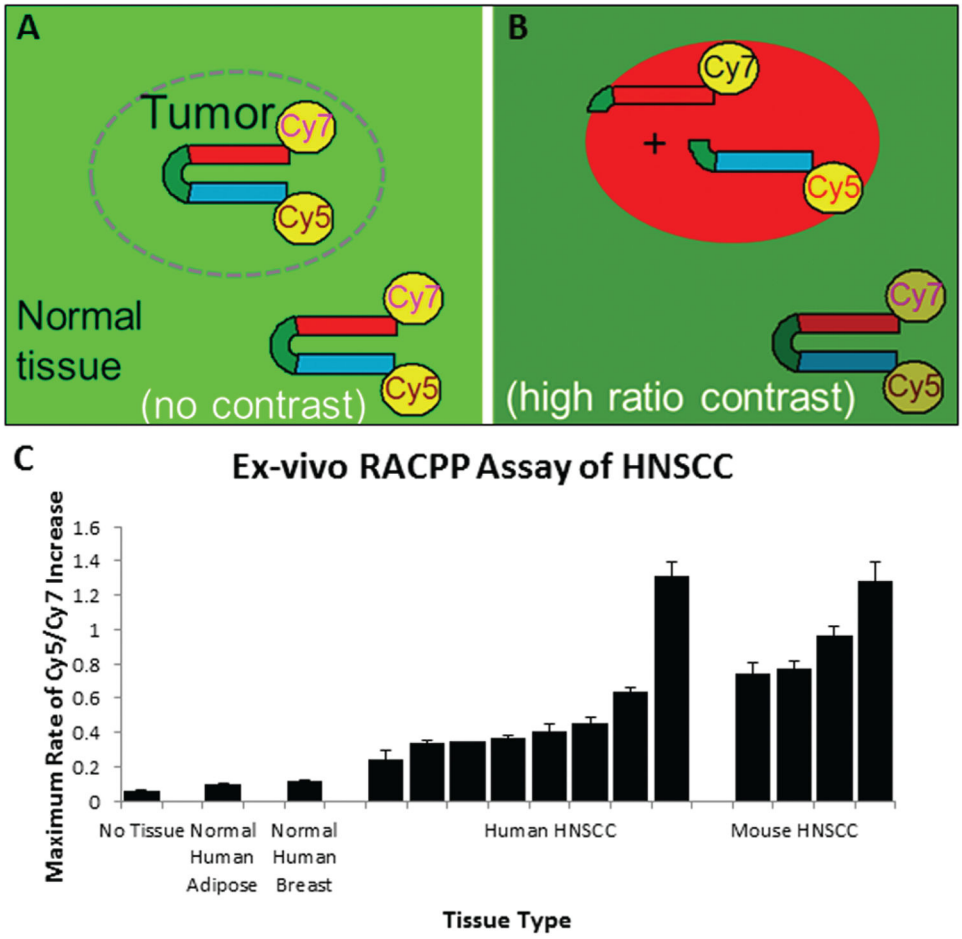

Figure 2.

RACPP schematic showing (A) no tumor-contrast immediately post-injection; (B) high tumor-contrast following MMP-dependent cleavage, separating Cy5 from Cy7. (C) Application of RACPP to HNSCC specimens produces faster Cy5/Cy7 ratio change compared to normal tissue. Abbreviations: RACPP, ratiometric activatable cell-penetrating peptide; HNSCC, head and neck squamous cell carcinoma.

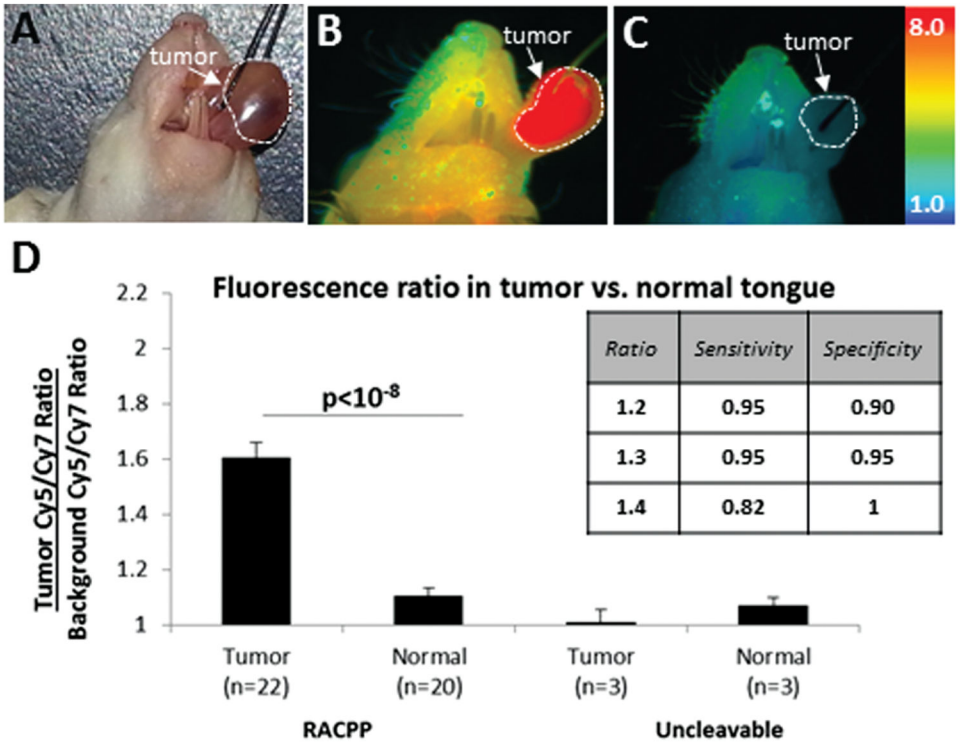

Figure 3.

(A, B) RACPP injection produces greater ratiometric fluorescent signal in HNSCC tumor versus normal tissue. (C) Uncleavable-control does not produce tumor-specific contrast. (D) RACPP is sensitive and specific for tumor detection. Abbreviations: HNSCC, head and neck squamous cell carcinoma; RACPP, ratiometric activatable cell-penetrating peptide.

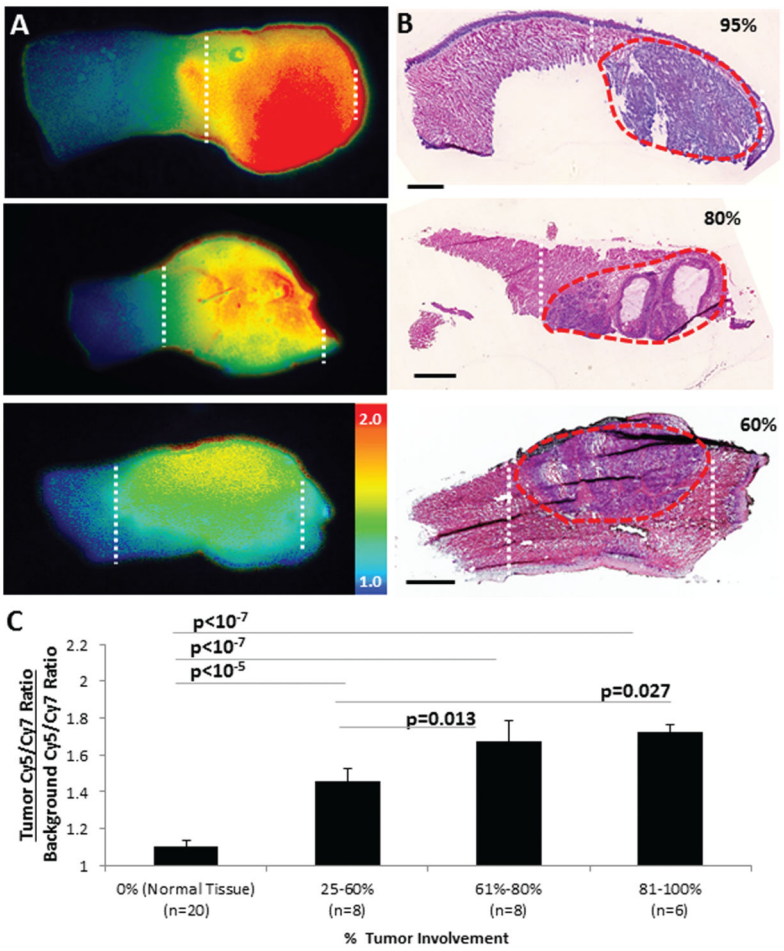

Figure 4.

(A) Ratiometric images showing higher fluorescence in tumor (white stippling). (B) Corresponding H&E images confirming tumor burden (red stippling). (C) Ratiometric activatable cell-penetrating peptide (RACPP) uptake correlates directly with tumor burden.